DYNAMO ACTION IN PRECESSING CYLINDERS

NORE[1] C., LEORAT[2] J., GUERMOND[3] J.-L., CAPPANERA[1] L., LUDDENS[1,4] F.
[1]*LIMSI-CNRS/*Bâtiment 508, BP 133, 91403 Orsay cedex, France et Université Paris-Sud, 91405 Orsay cedex, France, [2]*Luth*, Observatoire de Paris-Meudon, place Janssen, F-92195-Meudon, France, [3]Department of Mathematics, Texas A&M University, 3368 TAMU, College Station, Texas 77843-3368, USA,
[4]*IMB* Université Bordeaux I, 351 cours de la Libération, 33405 Talence cedex, France.
E-mail address of corresponding author: caroline.nore@limsi.fr

Abstract : It is numerically demonstrated by means of a magnetohydrodynamic (MHD) code that precession can trigger dynamo action in a cylindrical container. Fixing the angle between the spin and the precession axis to be $\pi/2$, two configurations of the spinning axis can be explored: either the symmetry axis of the cylinder is parallel to the spin axis (this configuration is henceforth referred to as the *axial spin* case), or it is perpendicular to the spin axis (this configuration is referred to as the *equatorial spin* case). In both cases, when the Reynolds number, based on the radius of the cylinder and its spin angular velocity, increases, the flow, which is initially centro-symmetric, loses its stability and bifurcates to a quasi-periodic motion. This unsteady and asymmetric flow is shown to be capable of sustaining dynamo action in the linear and nonlinear regimes. The magnetic field thus generated is mainly quadrupolar in the *axial spin* case while it is mainly dipolar in the *equatorial spin* case. These numerical evidences of dynamo action in a precessing cylindrical container may be useful for the design of new dynamo experiments, such as the one planned at the DRESDYN facility in Germany [1].

1. Introduction

The idea that precession can be a potent mechanism to drive dynamo action has long been debated (see for example [2]). Modern astrophysical observations of some planetary dynamos can contribute to resolving this issue, although definite evidence is still lacking. Because of the large computing resources required, it is only recently that numerical computations have demonstrated that dynamo action occurs in different precessing containers: spherical [3] and spheroidal [4] ones. Since neither spheres nor spheroids are convenient for large-scale experiments, it is instructive to investigate whether similar results can be obtained in cylindrical containers. The purpose of the present paper is to report results from our investigating this issue by using a nonlinear magnetohydrodynamic (MHD) code called SFEMaNS (for Spectral / Finite Elements for Maxwell and Navier-Stokes equations, [5]). This code solves the nonlinear MHD equations for incompressible fluids in heterogenous domains (with spatial distributions of electrical conductivity or magnetic permeability) composed on conducting and non-conducting parts. SFEMaNS is spectral in the azimuthal direction and uses finite elements in meridional section (see [6] for more details). Six parameters govern the flow: the aspect ratio of the container, the precession angle (angle between the spin axis OS and the precession axis OP), the spin angle (angle between the symmetry axis OZ and the spin axis OS), the precession rate ε (ratio of the precession and spin angular velocity), the Reynolds number Re and the magnetic Reynolds number Rm (see fig. 1). Choosing the container height equal to its diameter, the precession axis orthogonal to the spin axis (precession angle is $\pi/2$) and the precession rate $\varepsilon=0.15$, we are left with two limit configurations: one called *axial spin* for which the spin angle is 0 and the symmetry axis of the cylinder remains fixed in the precession frame (see fig. 1 right) and another one called

equatorial spin for which the spin angle is π/2 and the symmetry axis rotates in the precession frame (see fig. 1 left). We focus our attention on these two configurations because, in the *axial spin* case, the wall speed is tangent to the wall and only the viscous stress on the wall drives the flow while, in the *equatorial spin* case, the flow is driven by the pressure on the wall and is therefore inertially driven. The MHD equations solved by SFEMaNS are written:

$$\partial_t \mathbf{u} + (\mathbf{u}\cdot\nabla)\mathbf{u} + 2\varepsilon \mathbf{e}_p \times \mathbf{u} + \nabla p = \frac{1}{R_e}\Delta\mathbf{u} + \mathbf{f},$$
$$\nabla\cdot\mathbf{u} = 0,$$
$$\partial_t \mathbf{h} - \nabla\times(\mathbf{u}\times\mathbf{h}) = \frac{1}{R_m}\Delta\mathbf{h},$$
$$\nabla\cdot\mathbf{h} = 0,$$

where **u**, p and **h** are the velocity field, the pressure and the magnetic field, respectively. **f** is the Lorentz force.

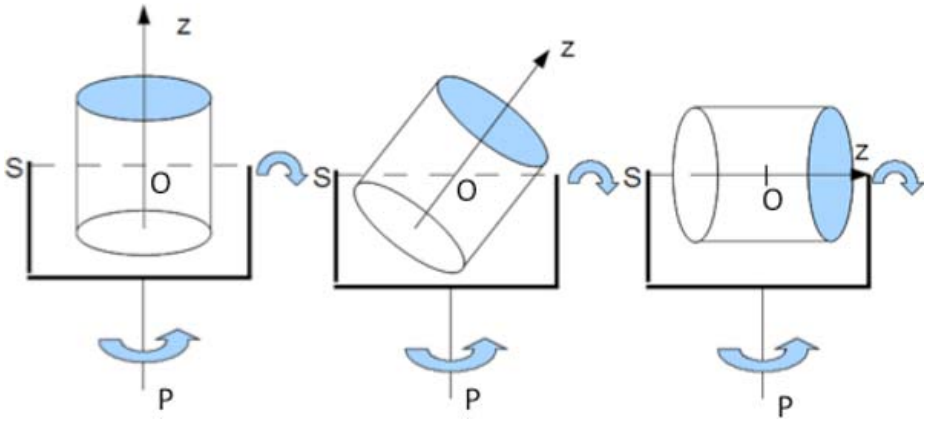

Figure 1: Different configurations for precession driving: (left) equatorial spin (the spin angle is π/2); (middle) oblique spin; (right) axial spin (the spin angle is 0). OS is the spin axis, OP the precession axis and OZ the symmetry axis.

2. Hydrodynamic study

In this section we examine the two configurations in the hydrodynamic regime, where Re is the control parameter. At low Reynolds number, the flow is steady and centro-symmetric, meaning that **u**(**r**)=-**u**(-**r**). At larger Reynolds numbers, the loss of centro-symmetry can be monitored by inspecting the symmetric and antisymmetric components of the velocity field: $\mathbf{u_s}(\mathbf{r},t) = (\mathbf{u}(\mathbf{r},t)-\mathbf{u}(-\mathbf{r},t))/2$ and $\mathbf{u_a}(\mathbf{r},t) = (\mathbf{u}(\mathbf{r},t)+\mathbf{u}(-\mathbf{r},t))/2$. In the Navier-Stokes simulations reported here, we monitor the time evolution of the total kinetic energy $K(t) = 0.5 \int \mathbf{u}^2\, dV$ and that of the asymmetric kinetic energy $Ka(t) = 0.5 \int \mathbf{u_a}^2\, dV$. The time evolution of these two quantities are reported in Figure 2 in the two cases configurations. For the *axial spin* case, the efficiency of the viscous forcing decreases when Re increases; for the *equatorial spin* case, saturation is not achieved yet at Re = 2000, (see left panel). The asymmetry ratio is larger in the *equatorial spin* case than in the *axial spin* case (see right panel). Based on the phenomenological argument that dynamo action is favored by symmetry breaking, it could be anticipated that the *equatorial spin* case would generate dynamo action at a lower threshold than the *axial spin* case. However, it is shown below that this intuitive argument is incorrect.

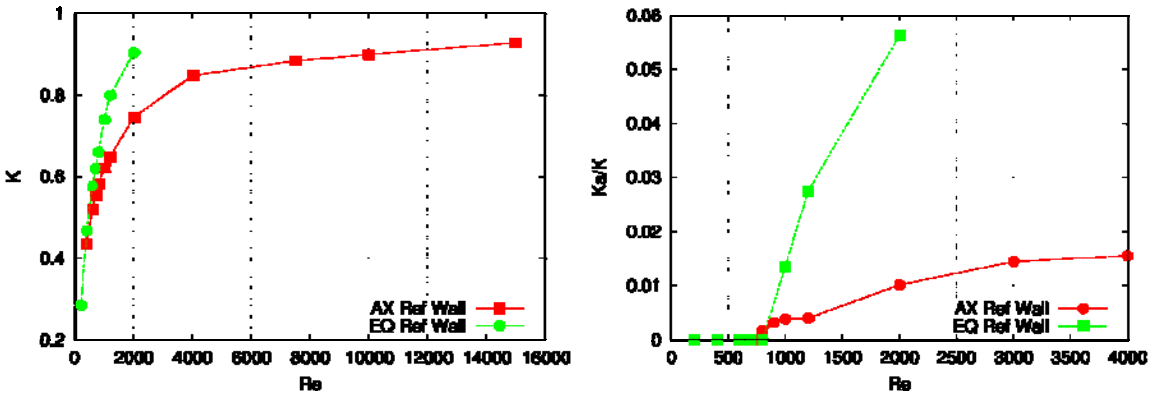

Figure 2: Comparisons between the axial and equatorial spin cases in the reference frame of the wall (also called the *mantle frame*) for a fixed precession rate 0.15: (left) total kinetic energy as a function of Re; (right) asymmetry ratio Ka(t)/K(t) as a function of Re.

3. Dynamo action

We now investigate the MHD regime, where Re and Rm are the two control parameters. The nonlinear MHD simulations use a small magnetic seed field as initial data or restart from a state computed at neighboring parameters. As already observed for spherical and spheroidal dynamos, dynamo action occurs after symmetry breaking of the flow when the magnetic dissipation is small enough, i.e. for magnetic Reynolds numbers Rm above a critical value $Rm_c(Re)$.

In the *axial spin* case, we have found [7] that $Rm_c \approx 750$ at Re = 1200. The generated magnetic field is unsteady and mainly quadrupolar. The computed critical curve $Rm_c(Re)$ is shown in Figure 3. The critical magnetic Reynolds number is not a monotonic function of Re; there is a minimum value at Re = 1200. It seems that increasing Re leads to an efficiency reduction of the dynamo.

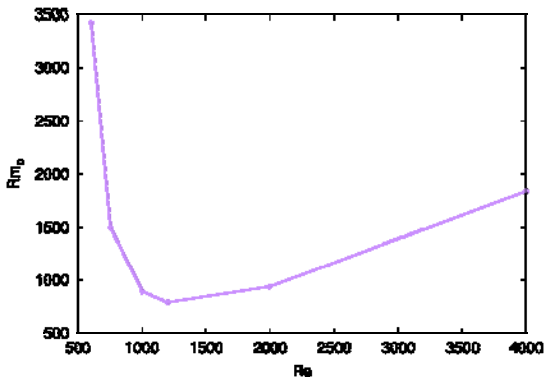

Figure 3: Critical curve $Rm_c(Re)$ in the *axial spin* case.

In the *equatorial spin* case, various MHD runs are performed at Re=1200 for different values of the magnetic Reynolds numbers Rm. The onset of dynamo action is monitored by recording the time evolution of the magnetic energy in the conducting fluid $M(t)= 0.5 \int \mathbf{h}^2 \, dV$. Two types of simulations are done: linear dynamo runs are first performed by imposing $\mathbf{f} = 0$ in the Navier-Stokes equations, i.e. the retroaction of the Lorentz force on the velocity field is

disabled, then the Lorentz force **f** is restored in the Navier-Stokes equations to observe the nonlinear saturation.

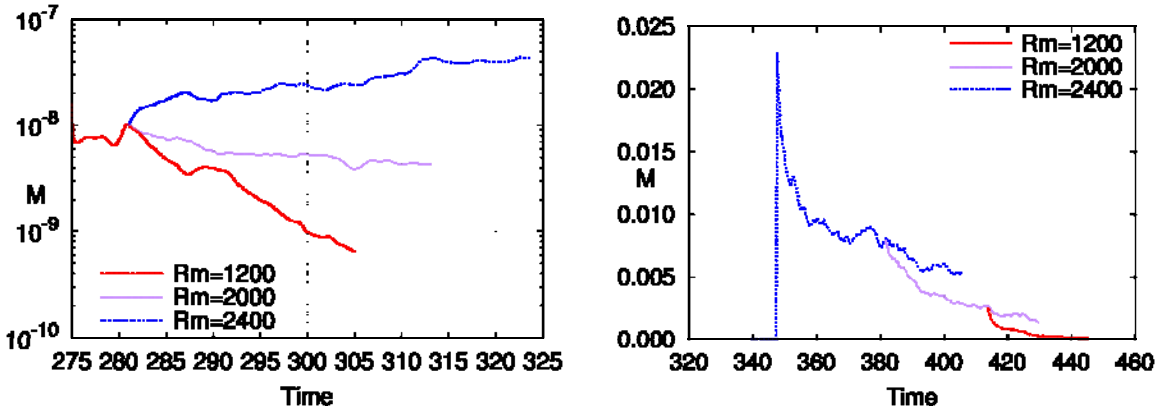

Figure 4: Time evolution of the magnetic energy M in the conducting fluid (left) in the linear regime from t = 275 at Re = 1200 and various Rm as indicated (in lin-log scale) and (right) in the nonlinear regime for Re = 1200 and various Rm as indicated. *Equatorial spin* case.

(1) A first series of linear dynamo simulations is done with Rm=1200, 2000 and 2400. The time evolution of M is shown in Figure 4 (left). The initial velocity and magnetic field for the runs at Rm=2000 and 2400 are the velocity and the magnetic fields obtained from the run at Rm=1200 at t=282. Dynamo action occurs when M(t) is an increasing function of time for large times with a positive growthrate (as is the case for Rm=2400). Linear interpolation of the growthrates gives the critical magnetic Reynolds number $Rm_c \approx 2130$ at Re=1200, i.e. the critical magnetic Reynolds number is almost three times larger than that in the *axial spin* case.

(2) To observe the nonlinear saturation (the Lorentz force **f** is restored in the Navier-Stokes equations), we use as initial data the velocity and magnetic fields from the linear MHD run at t=346 for Rm=2400. The amplitude of the initial magnetic field is multiplied by 400 to reach saturation faster; the initial velocity field is kept unchanged. Figure 4 (right) shows that M decreases rapidly over a time period corresponding to one turnover time, i.e. until t=352, and begins to oscillate thereafter. After restarting the MHD run at t=382 with Rm=2000 and running it until t=428, we observe that M decreases. After restarting the MHD run at t=412 with Rm=1200 and running it until t=446, we observe that the dynamo dies in a short time lapse. A snapshot of the vorticity and the magnetic field lines at Re=1200 and Rm=2400 is shown on fig. 5. We observe a central S-shaped vortex deformed by the precession and connected to the walls through viscous boundary layers. The magnetic energy is dominated by the azimuthal modes m=1, 2, 3 and the magnetic field lines exhibit a dominant dipolar shape.

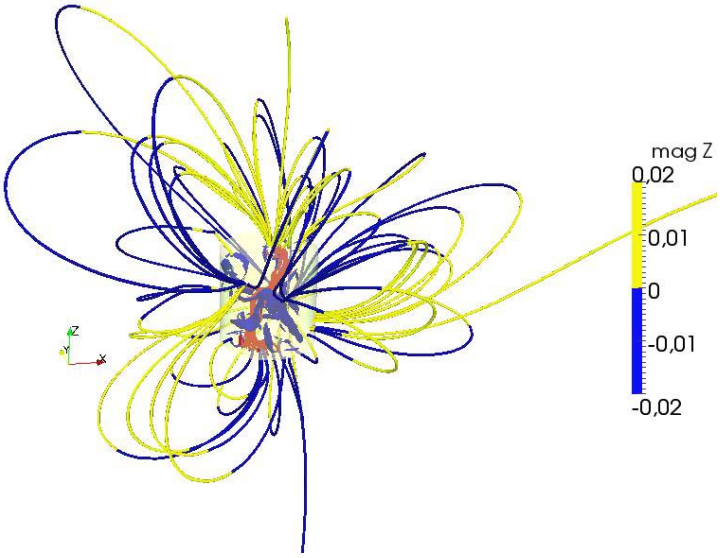

Figure 5: Snapshot at Re=1200 and Rm = 2400 of the vorticity field lines (grey/red) and the magnetic field lines colored by the axial component (light grey/yellow for positive vertical magnetic field component and black/blue for negative vertical magnetic field component). The view is seen from the side (Ox is the spin axis, Oz the precession axis). *Equatorial spin* case.

4. Conclusion

We have studied the dynamo capabilities of a precessing cylinder in two limit configurations. The dynamo threshold found in the *equatorial spin* configuration is larger than that found in the *axial spin* configuration at the same Reynolds number Re=1200. This result contradicts the intuition that wall-normal stress would enhance symmetry breaking and would favor dynamo action. The challenge is now to increase the Reynolds numbers in the MHD simulations to more realistic values.

5. References

[1] Stefani, F., Eckert, S., Gerbeth, G., Giesecke, A., Gundrum, Th., Steglich, C., Weier, T., Wustmann, B. DRESDYN - A new facility for MHD experiments with liquid sodium. Magnetohydrodynamics 48, 103-113, 2012 .

[2] W. V. R. Malkus. Precession of the Earth as the cause of geomagnetism: Experiments lend support to the proposal that precessional torques drive the Earth's dynamo. Science, 160(3825): 259–264, 1968.

[3] A. Tilgner. Precession driven dynamos. Physics of Fluids, 17(3):034104, 2005.

[4] C.-C. Wu and P. Roberts. On a dynamo driven by topographic precession. Geophysical & Astrophysical Fluid Dynamics, 103(6):467–501, 2009.

[5] J.-L. Guermond, R. Laguerre, J. Léorat, and C. Nore. Nonlinear magnetohydrodynamics in axisymmetric heterogeneous domains using a Fourier/finite element technique and an interior penalty method. J. Comput. Phys., 228:2739–2757, 2009.

[6] J. L. Guermond, J. Léorat, F. Luddens, C. Nore and A. Ribeiro, Effects of discontinuous magnetic permeability on magnetodynamic problems, J. Comp. Physics 230, 6299–6319, 2011.

[7] C. Nore, J. Léorat, J. L. Guermond and F. Luddens, Nonlinear dynamo action in a precessing cylindrical container, Physical Review E 84, 016317, 2011.